# Profile Flags: a Novel Metaphor for Probing of $T_2$ Maps

Matej Mlejnek[*], Pierre Ermes[†], Anna Vilanova[‡],
Rob van der Rijt[§], Harrie van den Bosch[§], Frans Gerritsen[†], and Meister Eduard Gröller[*]

[*]Institute of Computer Graphics and Algorithms, Vienna University of Technology, Austria
[†]Philips Medical Systems, Best, Netherlands
[‡]Department of Biomedical Engineering, Technische Universiteit Eindhoven, Netherlands
[§]Catharina Hospital, Eindhoven, Netherlands
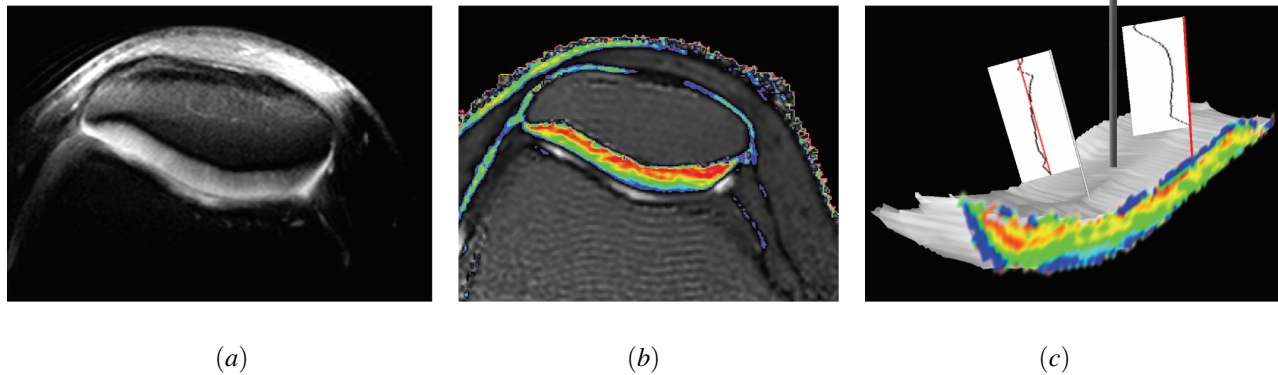
(a)　　　　　　　　　　(b)　　　　　　　　　　(c)

Figure 1: One slice of an anatomical scan of a patella (a) and the corresponding $T_2$ map (b) of articular cartilage investigated with Profile Flags (c).

## ABSTRACT

This paper describes a tool for the visualization of $T_2$ maps of knee cartilage. Given the anatomical scan and the $T_2$ map of the cartilage, we combine the information on the shape and the quality of the cartilage in a single image. The Profile Flag is an intuitive 3D glyph for probing and annotating of the underlying data. It comprises a bulletin board pin-like shape with a small flag on top of it. While moving the glyph along the reconstructed surface of an object, the curve data measured along the pin's needle and in its neighborhood are shown on the flag. The application area of the Profile Flag is manifold, enabling the visualization of profile data of dense but inhomogeneous objects. Furthermore, it extracts the essential part of the data without removing or even reducing the context information. By sticking Profile Flags into the investigated structure, one or more significant locations can be annotated by showing the local characteristics of the data at that locations. In this paper we are demonstrating the properties of the tool by visualizing $T_2$ maps of knee cartilage.

**CR Categories:** I.3.8 [Computing Methodologies]: Computer Graphics—Applications; J.3 [Computer Applications]: Life and medical sciences—Medical information systems

**Keywords:** visualization in medicine, applications of visualization

## 1 INTRODUCTION AND MEDICAL BACKGROUND

The surfaces of knee joints are covered by a tissue with a complex structure, called articular cartilage. Among the functions of the cartilage are distribution of weight, frictionless motion and shock absorption. Damage to the cartilage can be either post-traumatic or degenerative, both may lead to osteoarthritis. In osteoarthritis, softening of the cartilage is observed, causing the tissue to be less resistant to load bearing. Ulceration and thinning of the cartilage occurs in the next stage of osteoarthritis, leading to exposure of the bear bone in the course of several years. Clinically, this is accompanied by pain, stiffness and progressive loss of function. Research to find treatments to stop or even reverse these degenerative changes are well in progress. Essential to a treatment at an early stage of osteoarthritis is early detection of cartilage degeneration [4, 8, 5].

Important factors in the characterization of cartilage degeneration are thickness of the tissue layer and tissue quality, the latter represented in water-content or $T_2$ values. Both are important for a quantitative and qualitative measurement, respectively, thus, allowing for follow up to the disease progression and to the response to treatment. Since the cartilage is only a few millimeters thick, an accurate measurement of the thickness and of the quality of the tissue is necessary for the early determination of a joint's degeneration. A change in cartilage thickness and its quality indicates the state of the disease and can be used, e.g., for the estimation of the progress
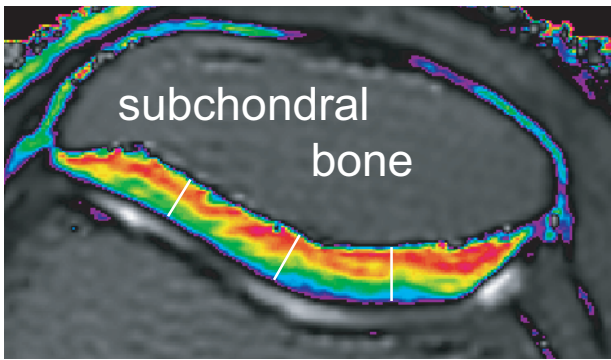
[*]{mlejnek|groeller}@cg.tuwien.ac.at
[†]{pierre.ermes|frans.gerritsen}@philips.com
[‡]A.Vilanova@tue.nl
[§]rob@vanderrijt.nl|harrie.vd.bosch@catharina-ziekenhuis.nl

Figure 2: $T_2$ map of the articular cartilage with three $T_2$ profiles (white lines). Notice their perpendicular alignment to the underlying subchondral bone.

of osteoarthritis, or for the evaluation of the response to therapies.

Current MR cartilage-imaging techniques allow a detailed examination of the joint cartilage, including both thickness and quality of the tissue. In general, two types of MR sequences are used: a high-resolution anatomical scan (e.g., a 3D water suppressed sequence or proton density weighted sequence) and a $T_2$ map, representing the tissue quality. The computation of $T_2$ maps from spin-echo images is discussed in section 3.1. Figures 1(a) and (b) show one slice of the anatomical scan and the $T_2$ map of the patellar cartilage, respectively. While the anatomical scan gives the information about the shape and thickness of the cartilage, in $T_2$ maps the radiologists are searching for disruptions of typical $T_2$ patterns. Therefore, these two scans are usually studied on two linked screens in a slice-by-slice manner or by multi-planar reconstruction for radiological assessment. This considerably reduces the spatial perception and prolongs the examination time. A 3D representation of the cartilage anatomy is a valuable tool for radiologists, giving added 3D information for a better localization of lesions. For a better communication with the orthopedists diagnostic information is illustrated in one single image with anatomic correlation. This allows an easy access to this information, for example during surgical procedures. Integration of qualitative information as provided by the $T_2$ map into the 3D representation makes a tool like this even more valuable.

Our approach deals with combining the anatomical information with the quality information of the cartilage. Although the knee is fixed during the acquisition, these two sequences have to be registered by an affine transformation. It is based on local correlations [19] to compensate slight patient's movements. Then, the surface of the articular cartilage is reconstructed from the high-resolution anatomical scan. In order to obtain the $T_2$ map limited to the interior of the cartilage, the previously computed segmentation mask is applied to the $T_2$ map.

Recently, the spatial distribution of the $T_2$ relaxation times within the cartilage has been widely discussed in medical literature [13, 14, 18, 12]. For the validation of the quality of the cartilage by means of disruptions in the $T_2$ map, so called $T_2$ profiles are calculated. A $T_2$ profile is the curve of varying $T_2$ values along a line that is perpendicular to the subchondral bone and ends at the surface of the cartilage (see figure 2). For healthy cartilage the $T_2$ profiles have a typical characteristic shape. This is due to the fact that for healthy cartilage the $T_2$ values are arranged in layers parallel to the subchondral bone. The $T_2$ profiles in lesion areas significantly deviate from these characteristic shapes. Multiple $T_2$ profiles can be generated in order to obtain local characteristics for comparison of different regions of the cartilage and comparison between specimens. Since several factors, e.g., the age or the physical proportions of the patients, are significant for the thickness and the $T_2$ relaxation times, a normalized profile can be computed. It yields the $T_2$ times for the normalized distances between the subchondral surface (distance 0.0) and the articular surface (distance 1.0). This enables a comparison of spatial variation of two profiles with different lengths.

The main contribution of this paper is the introduction of the Profile Flag, a novel user interface for investigating $T_2$ maps (see figure 1(c)). This glyph enables probing of the $T_2$ maps within the articular cartilage. It provides information about the thickness as well as the quality of the cartilage. The Profile Flag improves on two ineffective steps in the workflow of articular cartilage inspection in clinical practice. Firstly, by browsing the $T_2$ profiles on a reconstructed surface of the cartilage, the radiologist does not need to switch between two screens in order to observe both, the thickness changes and the quality within the cartilage. Moreover, by using multiple Profile Flags, the disruptions in the structure of the $T_2$ map and, thus the deviation from a "healthy" profile can be visualized in an intuitive way. Secondly, the commonly used procedure of communication between the radiologist and the orthopedist involves marking and printing out all slices including the identified lesion. Using the Profile Flag, the investigating radiologist can simply annotate the affected regions on a reconstructed surface by showing the local characteristics of the cartilage in one single image.

The paper is structured as follows. Related work on volumetric data interaction and annotation is reviewed in section 2. Then, the necessary environment for the visualization of the $T_2$ maps are sketched in chapter 3. In the central section 4 of the paper, we discuss the different setups of the Profile Flag. Results are shown in section 5. In chapter 6 we discuss possible extensions to the Profile Flag. Finally, we summarize and conclude the work in section 7.

## 2 RELATED WORK

There is a large body of work discussing the annotation of volumetric data. Every feature can be annotated by a rectangular caption, which is located outside the volume in image space. Each caption is assigned to one pre-defined feature in the data. Usually, the main issue of papers from this track is the arrangement of the rectangles with the purpose of avoiding overlap in image space [6]. Bell et al. [2] address the above mentioned issues in a virtual 3D environment. Several groups are discussing glyphs with picking and manipulating capabilities in virtual environments [17].

Recently, the use of advanced interaction tools is gaining popularity beyond what is already available in medical workstations. Besides the commonly used cutting planes (or even, arbitrary cutting objects), McGuffin et al. [10] presented an interactive tool for investigation of volumetric data based on different kinds of deformations and layerings of the objects. More application-specific glyphs have been presented by Huitema and van Liere [7] for molecular data, comprising translation and measurement capabilities. In Preim et al. [15], measures like distances or angles, can be determined by an intuitive interface.

In flow visualization, de Leeuw and van Wijk [3] present a glyph for the visualization of multi-dimensional data. The glyph can be located at an arbitrary position and it visualizes the local characteristics of several flow attributes.

In our previous work [11], we discuss the visualization of the thickness of femoral cartilage. Since the femoral cartilage constitutes a curved structure, we concentrate on visualizing the thickness information by unfolding the cartilage. In this paper we focus on the patellar cartilage, which is a flat structure when no lesions are present. Thus no deformations are necessary to represent the thickness in a reliable way. Moreover, given the current scan resolution, the patellar cartilage is thick enough for observing spatial variations
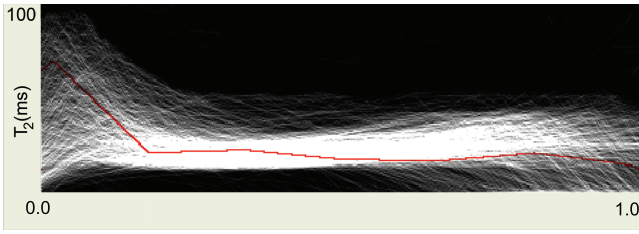
Figure 3: Spatial variation in $T_2$ as a function of normalized distance from the subchondral bone (0.0) to the articular surface (1.0) for the patella. The selected profile is depicted in red.

of the $T_2$ times within the cartilage.

## 3 CARTILAGE INVESTIGATION ENVIRONMENT

In this sections we shortly present two aspects, which are closely related to the investigation of the $T_2$ maps. First, the computation of the $T_2$ maps from a series of spin-echo images is described. In the second subsection, we discuss the graph of profiles, a depiction that provides statistical information by showing a series of profiles from all over the cartilage surface.

### 3.1 Computation of the $T_2$ map

As mentioned above, two MR acquisition sequences are used for the quantitative and qualitative measurements, respectively. The surface of the articular cartilage is generated from the anatomical scan, while the $T_2$ map is calculated from a sequence of spin-echo images. The $T_2$ map represents the tissue quality. A set of spin-echo images $M_i$ is acquired by varying the echo time $t_i$. Then, the $T_2$ map is calculated by fitting a non-linear mono-exponential curve on a voxel-by-voxel basis. The signal intensity of each voxel $V(j)$ of an image $M_i$ can be approximated by $V(j) \approx V_0(j) \cdot exp(\frac{-t_i}{T_2(j)})$, where $V_0(j)$ is the intensity of the voxel at echo time $t_i = 0$ and $T_2(j)$ is the relaxation time constant. We are fitting a curve through a weighted least squares approach. This is done by minimizing the sums of the squares of deviations between measured and expected values over all sequences: $min \sum_{i=0}^{N}(ln(V(j)) - ln(V_0(j)) + \frac{t_i}{T_2(j)})^2 w_i$. $N$ is the number of sequences and the $w_i$ are the weighting constants determining how strong the image $M_i$ affects the curve. The approach is chosen because of its high accuracy/computational cost ratio [9].

### 3.2 Graph of Profiles

A graph of profiles (see figure 3) is the first indicator of irregularities in the structure of the $T_2$ map. Since the shape of a $T_2$ profile is dependent on several factors like the age or the physical proportions of the patient, a default $T_2$ profile cannot be determined. Moreover, chemical shift artifacts at the bone/cartilage surface introduce longer $T_2$ values at this boundary. The shape of the curve thus depends on the segmentation technique [16]. Therefore, the graph of profiles is crucial to provide a statistical reference for the radiologists. A set of uniformly distributed profiles is computed for the entire surface starting from the subchondral bone. Each profile is shown in the graph in order to give an overview of all profiles. Such a simultaneous representation of many profiles discriminates the ones with suspicious characteristics as outliers. During browsing the profiles with the Profile Flag, the currently investigated profile is emphasized in red, while the remaining profiles yield a statistical information on the shapes of all the other $T_2$ profiles. Figure 3 shows a graph of profiles of a healthy specimen.
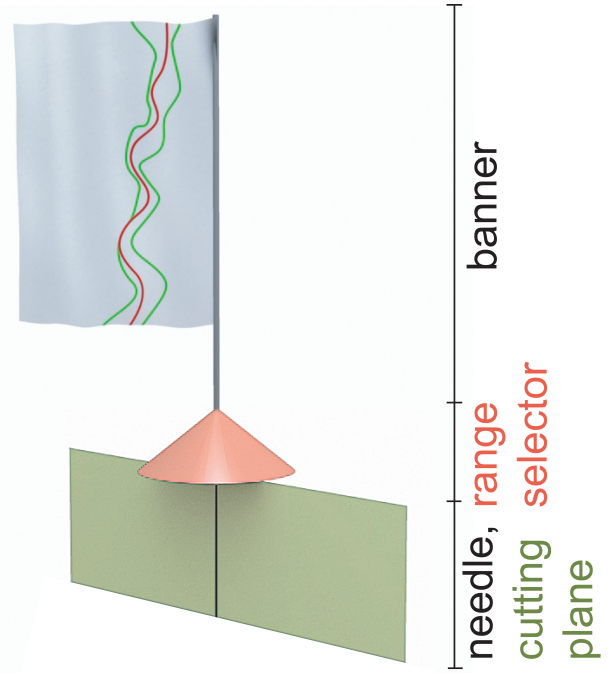


Figure 4: Profile Flag: a 3D glyph for probing of profiles. The glyph is located on the surface of the investigated structure, perpendicular to its surface. It consists of the banner, the range selector, the needle and the cutting plane.

## 4 PROFILE FLAG

So far, we have discussed the generation of the $T_2$ maps, which are investigated in a slice-by-slice manner in clinical practice. In this section we are presenting the Profile Flag for probing of the $T_2$ maps by browsing the reconstructed surface of the cartilage. The Profile Flag is a bulletin board pin-like interface for probing and annotating of underlying data. In order to visualize the corresponding profile, the Profile Flag is located on the surface of the cartilage. Since the $T_2$ profiles are defined along lines perpendicular to the subchondral bone interface, the Profile Flag is aligned with the normal vector of the surface at that position. During the investigation, one can drag the Profile Flag along the entire surface of the inspected object. Multiple Profile Flags can be stuck into the object in order to visualize multiple profiles or to emphasize the difference between two or more profiles. A Profile Flag consists of four components: the banner, the range selector, the needle and the cutting plane (see figure 4). In the following the components of the Profile Flag and interactions therewith are discussed.

### 4.1 The Needle

The needle is located beneath the surface of the inspected object. It defines the position of the reference profile. Two types of needles can be defined: a needle with a fixed length and a needle with an adaptable length. The fixed length needle samples the underlying volume at equally spaced intervals starting from the subchondral bone (see figure 5(a)). It yields the measured values in relation to the distance from the subchondral bone. In the investigation process of the cartilage, such a needle is designed for measuring the (absolute length) $T_2$ profiles. If a needle with an adaptable length is applied, the needle measures the normalized profile. It can be seen as a needle scaled to the thickness of the cartilage at the currently investigated point (see figure 5(b)).
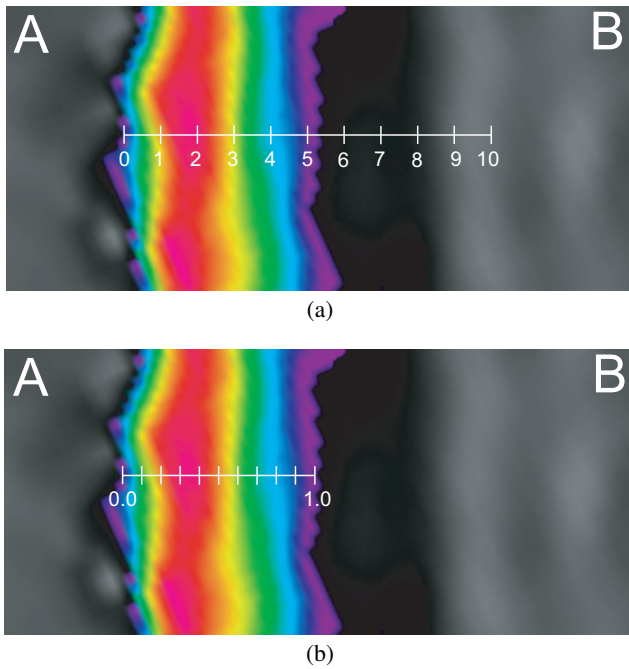
(a)



(b)

Figure 5: Two types of needles: (a) needle with a fixed length is probing the values at regularly spaced intervals and (b) an adaptive needle is sampling the measured values along the normalized distance from the subchondral bone A to the articular surface B.
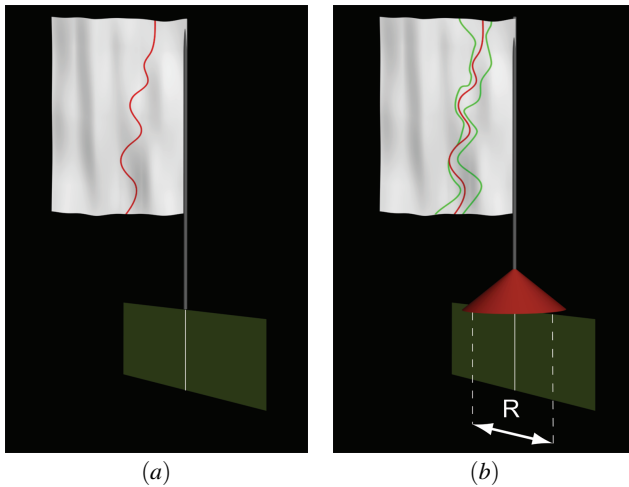


(a)                                    (b)

Figure 6: Two setups of the range selector. If the radius is set to 0 (a), only the reference profile is measured, setting $R > 0$ (b), all profiles within the neighborhood are visualized on the banner. The profile at the needle is shown in red. The green lines delimit all profiles in the neighborhood.

## 4.2   The Range Selector

The range selector enables the definition of the size of the investigated neighborhood. While the reference profile is defined by the position of the needle, the range selector determines the size of the interesting neighborhood through the radius $R$ of the cone. All profiles located within this range are visualized according to the type of the banner (see section 4.3). If the radius is set to 0, only the reference profile will be visualized (see figure 6).

## 4.3   The Banner

The banner represents the information defined by the position of the needle and the range defined by the range selector. For normalized profiles, the top of the banner corresponds to the subchondral surface, while the bottom of the banner corresponds to the articular surface (see figure 7). The banner is always facing the camera. This avoids projective distortions and thus distortions of the visualized information. On the banner the profile information is shown in one of several ways:

- **single profile banner**: by setting the radius $R$ to 0 only the reference profile at the needle is shown (see figure 8(a)).

- **single averaged profile banner** ($R > 0$): this type of banner averages all profiles within the radius R and shows only one averaged profile.

- **multiple profiles banner** ($R > 0$): in addition to the reference profile, all profiles within radius $R$ are taken into account. In order to avoid visual clutter by showing all profiles in the neighborhood, only the minimal and maximal values from all profiles are rendered in green (see figure 8(b), (c)). The green lines are not existing profiles but enclosure lines of all profiles in the investigated neighborhood.

- The **deviation profile banner** illustrates the difference of profiles from a reference profile. The reference profile is straightened and coincides with the vertical axis (see figure 8(d)). The other profiles undergo the same transformation. Thus the deviations from the reference profile are easily perceived. A deviation profile can be used to show the profile variance within a single neighborhood. Another possibility compares two different cartilage regions with two Profile Flags. The first Profile Flag defines the reference profile, e.g., in a healthy region. The second Profile Flag shows then the difference profiles in another (possibly suspicious) region (see figure 8(e)).

These banner types are a small collection of conceivable definitions of a set of profiles. Further possibilities include occurrence-based profile displays and reference profiles with statistical annotations (mean, variance).

## 4.4   Cutting Plane

The cutting-plane component of the Profile Flag is an extension of the multi-planar reconstruction, a tool which is usually applied for inspection of $T_2$ maps. Since we are primarily interested in those cross-sections of the data that include the reference profile, the needle should be included in the cutting plane. In order to investigate the entire neighborhood of the profile, the plane can be rotated by an arbitrary angle around the needle (see figure 9). Notice that, when the cutting plane is shown, the needle is not rendered in order not to hide the reference profile at the cross-section.

Moreover, the interaction with the reconstructed surface of the cartilage can facilitate the initial setting of the position and rotation of the desired cutting plane. Therefore, the cutting plane is defined by a point on the needle and a normal vector, independently from the rotation of the object. The normal vector of the plane has to be perpendicular to the direction vector of the needle. To choose the normal vector facing the camera, it should be located in the plane defined by the direction vector of the needle P and the viewing vector V. Thus, the normal vector can be calculated by $N = (V \times P) \times P$, where $V$ is the viewing vector from the camera to the location of the profile and $P$ is the direction vector of the needle.

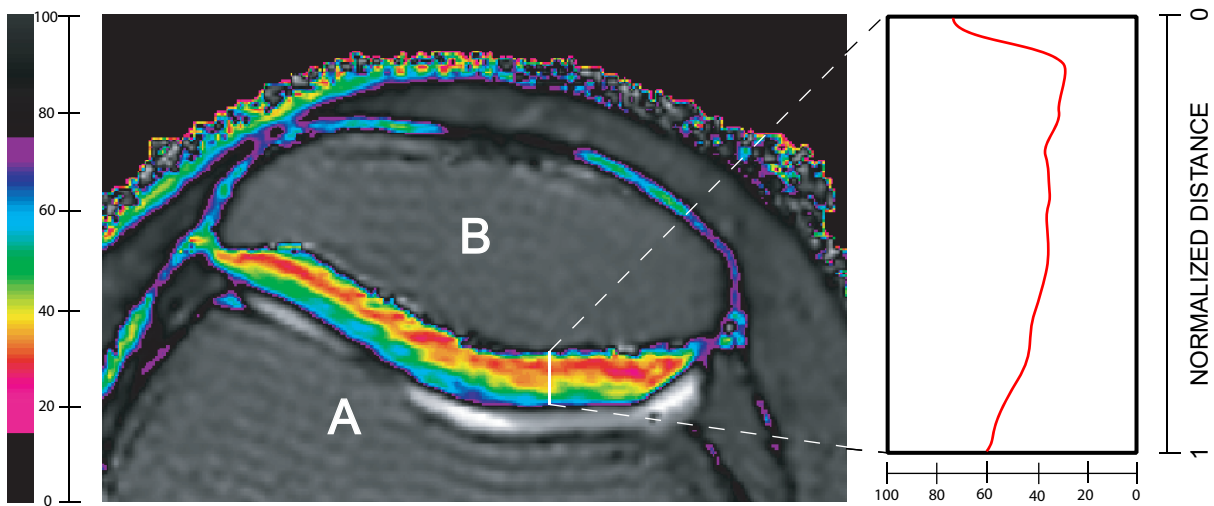The following two modes for interaction with the cutting plane are:

Figure 7: One slice of the $T_2$ map with one profile (left) and the corresponding banner (right). When measuring a normalized profile, the top of the banner (right) corresponds to the bone/cartilage (B) interface, while the bottom of the banner represents the articular surface (A).
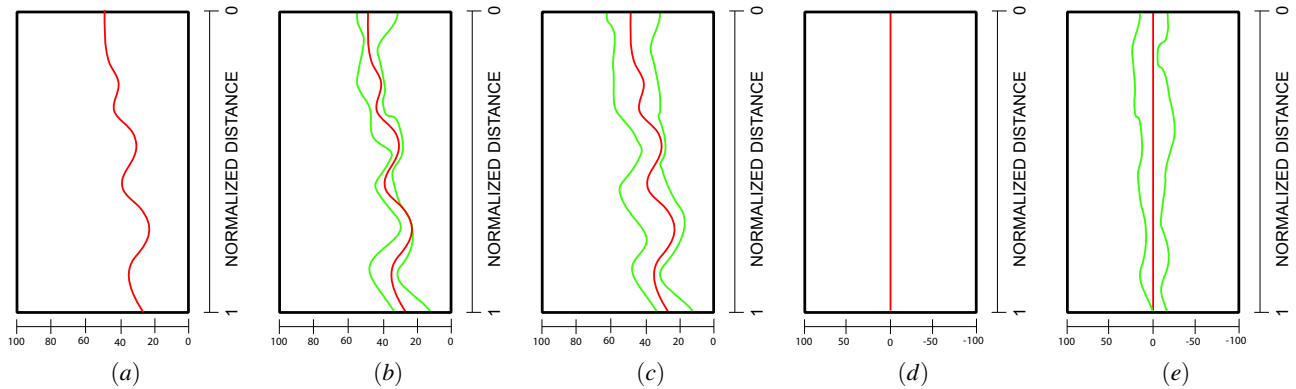


Figure 8: According to the type of the banner, the profiles defined by the needle and the range selector are visualized: (a) single profile banner, (b) multiple profiles banner (radius = 1mm), (c) multiple profiles banner (radius = 3mm), (d) deviation profile banner (radius = 0mm), (e) deviation profile banner (radius = 1mm).

- **rotation of the cutting plane around the needle**:
  This mode is convenient for rotation with small angles. The oblique position of the cutting plane produces projection distortions which grow with increasing rotation angle (see also figure 9(c) and (d)).

- **rotation of the object around the needle**:
  The second mode is designed for rotation with an arbitrary angle. The cutting plane remains parallel to the image plane and does not change its position in image space during the interaction. One can easily observe the entire neighborhood of the current profile. On the other side, a disorientation may occur while rotating the clipped reconstructed surface (see also figure 9(e) and (f)).

## 5   RESULTS

In this chapter we shortly discuss three scenarios of data annotations with the previously described Profile Flag. Figure 10 shows two possibilities of annotations of the quality of articular cartilage. Figure 10(a) contains two Profile Flags visualizing a healthy (left) and a suspicious profile (right). Moreover the left Profile Flag can

be set as a reference Profile Flag (figure 10(b)). Then, the right Profile Flag measures the deviations to the profile defined by the reference Profile Flag. Figure 11 visualizes also the profiles in the neighborhood of the reference profile. Notice, that while the reference Profile Flag visualizes the minimal and maximal $T_2$ values within the defined area, the right Profile Flags depicts the minimal and maximal deviation from the reference Profile Flag. An arbitrary number of Profile Flags can be stuck into the surface of the investigated object. Figure 12 shows an articular cartilage with three annotated profiles. The middle one defines the cutting plane, which shows a cross-section of the $T_2$ map including the profile defined by the reference profile.

## 6   DISCUSSION

The basic concept of the Profile Flags offers many opportunities. Here we discuss some of the possible extensions and applications of the Profile Flag.

- **Profile Flag as an Annotation Tool**
  By sticking one or more Profile Flags into the inspected structure, one can easily annotate regions of the object, which con-
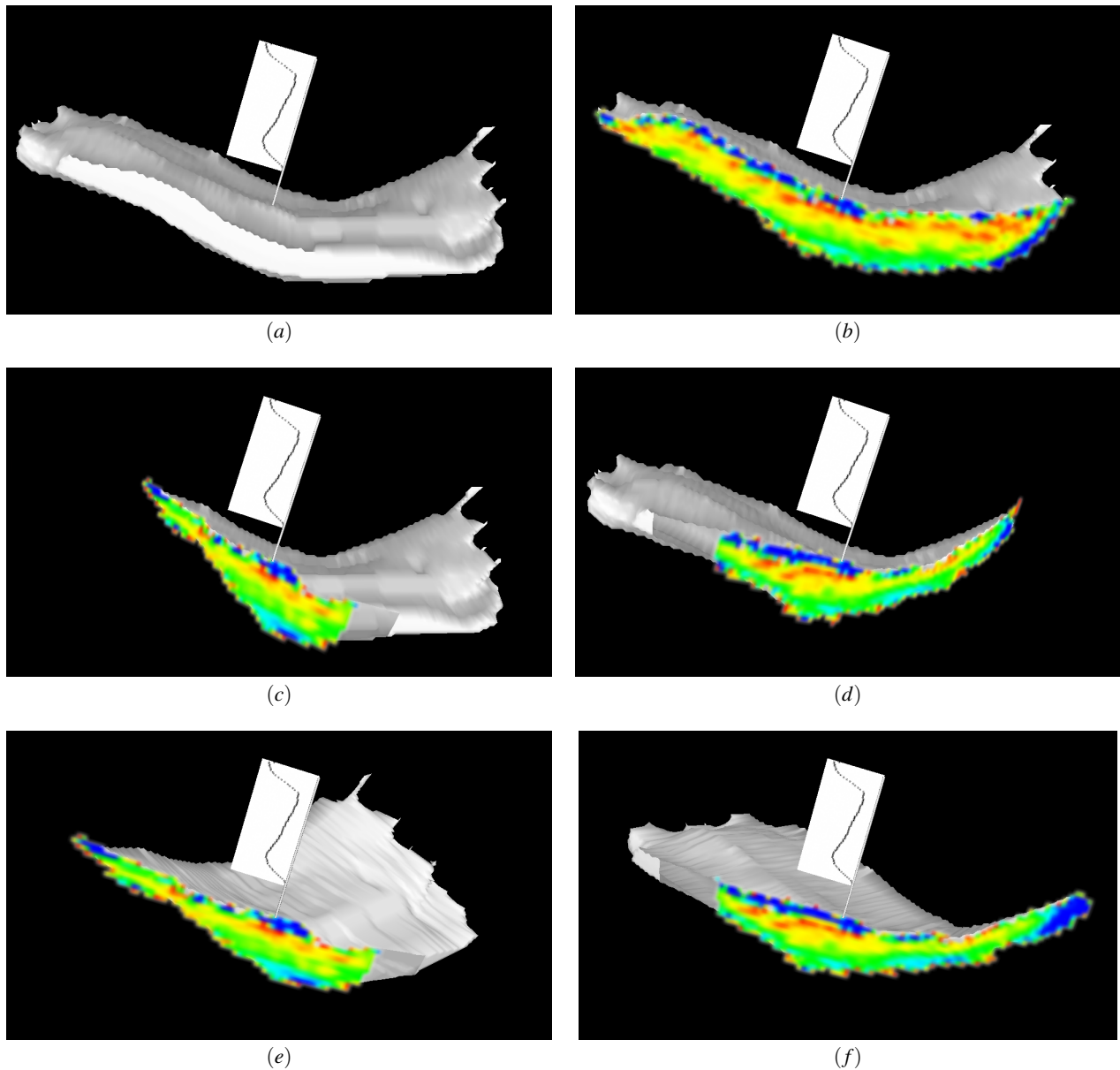
603

Figure 9: The reconstructed surface (a) of the articular cartilage including one Profile Flag. The cutting plane (b) is generated by taking into account the viewing vector and the needle position of the observed profile. Figures (c) and (d) demonstrate the rotation of the cutting plane around the needle at $+40$ and $-40$ degrees, respectively. Notice the distortion of the resulting $T_2$ map caused by the rotation. Figures (e) and (f) show the rotation of the reconstructed surface around the needle at $+40$ and $-40$ degrees, respectively. The cutting plane remains parallel to the image plane.

tain suspicious internal characteristics. In clinical practice, this step is crucial for transmitting the diagnosis from the inspecting radiologist to the orthopedist, who is performing the arthroscopy. This can be achieved in an efficient way by highlighting the damaged regions of the object in conjunction with the anatomical context.

- **Automatic Positioning of Profile Flags**
  Additionally to browsing the profiles, one can think of an automatic positioning of the Profile Flags. This can be a pre-processing step before starting the investigation of the structure. In case of cartilage imaging, one profile, comprising a healthy behavior, can be determined. The following investigation of the cartilage would include the browsing of the carti-

lage with the deviation profiles, which show only the variation from the reference profile. This step would involve a sophisticated statistical analysis, since the $T_2$ profiles differ among the population.

- **Seeding of Profiles**
  When inspecting an object with a curved surface, one can easily miss a profile with an important characteristic. This is particularly the case when using the Profile Flag for probing of profiles within a certain neighborhood. Thus, the density of the Profile Flags should be adapted to the curvature of the surface in order not to miss any area. A similar issue has been discussed by Vilanova et al. [1] for virtual colonoscopy.
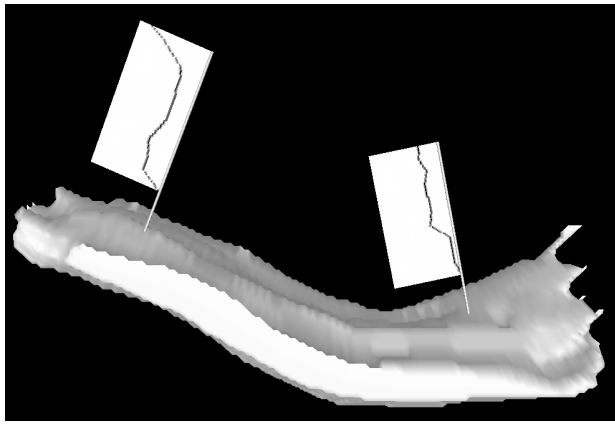
(a)
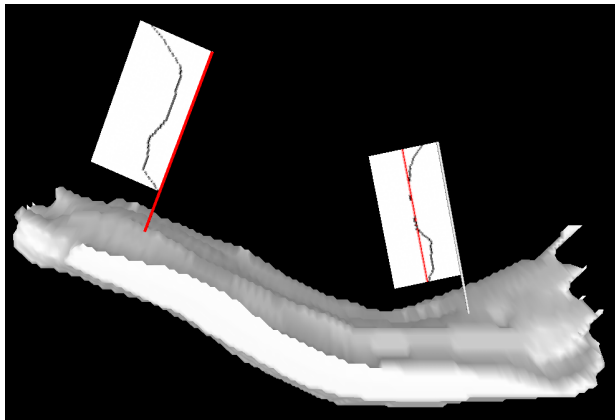


(b)

Figure 10: A disruption (right Profile Flag) in the pattern of the $T_2$ map can be annotated in two ways. Figure (a) shows two Profile Flags, where the left one show a healthy profile, while the right Profile Flag shows a suspicious profile. On the other hand, the left Profile Flag in figure (b) is set as a reference Profile Flag. The right one shows the deviation of the probed profile from the reference Profile Flag.

- **Restriction of Profiles**
  Additionally, the set of selected profiles can be restricted by a certain condition. For instance, restricting the maximum deviation for the multiple profile banner in any point causes a reduction in the number of profiles to the ones, which fulfill this criterion. This could involve modification of the shape of the range selector by pointing only to a subset of all previously selected profiles.

- **Application Areas**
  In this paper we demonstrate the use of Profile Flags for probing of $T_2$ maps. However the application of the tool is not limited to the investigation of knee cartilage. Other areas include visualization of 3D structures which have spatial or temporal curves associated to each 3D location. Examples include dense geologic data or time dependent series of dynamic contrast enhanced MRI for mammography.

## 7 SUMMARY AND CONCLUSIONS

In this paper we have presented the Profile Flag - a glyph for probing of underlying curve data. The Profile Flag consists of four com-
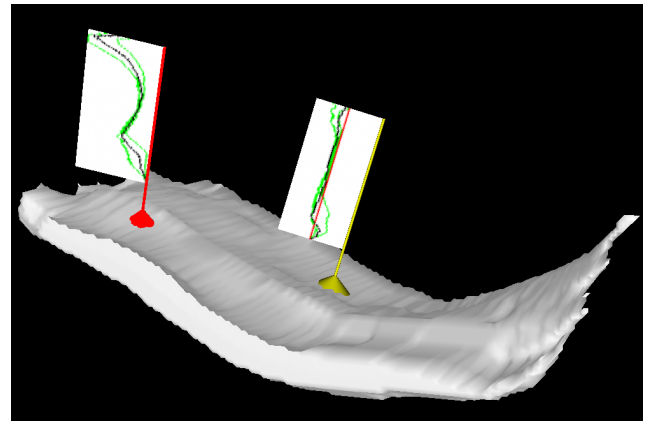


Figure 11: The reference Profile Flag (red) is located at a position of a healthy profile. Additionally, the extent of the profiles within the selected range is shown. The right profile (yellow) is showing the deviations from the reference Profile Flag. Again, the neighborhood of the current profile is visualized.
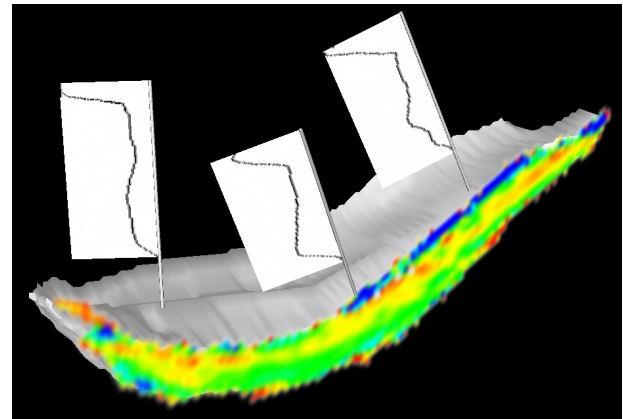


Figure 12: A $T_2$ map annotated by three Profile Flags stuck into the reconstructed surface of the articular cartilage. A cutting plane is showing a cross-section of the $T_2$ map of the Profile Flag in the middle.

ponents: the banner, the range selector, the needle and the cutting plane. It can be moved along the reconstructed surface of the cartilage by giving immediate feedback on the local characteristics of the underlying data. Since the essential information is rendered outside the investigated structure, there is no need to reduce the information about the shape or anatomy of the inspected object. Moreover, several regions of the object can be annotated, by using either the absolute or the relative representation of the measured quantity. We have presented the application of the Profile Flag in a medical environment for the investigation of knee cartilage. Besides observing the shape and the thickness of the cartilage, the radiologist can inspect the change in the quality of the cartilage by probing of the $T_2$ maps. The result of the inspection is the reconstructed surface of the object with annotated lesions, which can be easily interpreted by the orthopedist. The application of the Profile Flag is not restricted to a medical domain. Other applications areas include probing of curve data in structures, where the reduction of the context information is undesirable.

## REFERENCES

[1] A. Vilanova Bartroli, R. Wegenkittl, A. König, E. Gröller, and E. Sorantin. Virtual colon flattening. In *VisSym 2001 Joint Eurographics - IEEE TCVG Symposium on Visualization*, pages 127–136, 2001.

[2] Blaine Bell, Steven Feiner, and Tobias Höllerer. View management for virtual and augmented reality. In *Proceedings of the 14th annual ACM symposium on user interface software and technology*, pages 101–110, 2001.

[3] Willem C. de Leeuw and Jarke J. van Wijk. A probe for local flow field visualization. In *Proceedings of IEEE Visualization 1993*, pages 39–45, 1993.

[4] D. G. Disler, M. P. Recht, and T. R. McCauley. MR imaging of articular cartilage. *Skeletal Radiology*, 29:367–377, 2000.

[5] A. Guermazi, S. Zaim, B. Taouli, Y. Miaux, Ch. G. Peterfy, and H. K. Genant. MR findings in knee osteoarthritis. *European Radiology*, 13:1370–1386, 2003.

[6] Knut Hartmann, Bernhard Preim, and Thomas Strothotte. Describing abstraction in rendered images through figure captions. *Linkping Electronic Articles in Computer and Information Science*, 4(15), 1999.

[7] Henk Huitema and Robert van Liere. Interactive visualization of protein dynamics. In *Proceedings of IEEE Visualization 2000*, pages 465–468, 2000.

[8] H. Imhof, I.-M. Nöbauer-Huhmann, C. Krestan, A. Gahleitner, I. Sulzbacher, S. Marlovits, and S. Trattnig. MRI of the cartilage. *European Radiology*, 12:2781–2793, 2002.

[9] James R. MacFall, Stephen J. Riederer, and Henry Z. Wang. An analysis of noise propagation in computed $T_2$, pseudodensity and synthetic spin-echo images. *Medical Physics*, 13(3):285–292, 1986.

[10] Michael J. McGuffin, Liviu Tancau, and Ravin Balakrishnan. Using deformations for browsing volumetric data. In *Proceedings of IEEE Visualization 2003*, pages 401–408, 2003.

[11] Matej Mlejnek, Anna Vilanova, and Meister Eduard Gröller. Interactive thickness visualization of articular cartilage. In *Proceedings of IEEE Visualization 2004*, pages 521–527, oct 2004.

[12] Timothy J. Mosher, Christopher M. Collins, Harvey E. Smith, Lauren E. Moser, Rebecca T. Sivarajah, Bernard J. Dardzinski, and Michael B. Smith. Effect of gender on in vivo cartilage magnetic resonance imaging T2 mapping. *J. Magn. Reson. Imaging*, 19:323–328, 2004.

[13] Timothy J. Mosher, Bernard J. Dardzinski, and Michael B. Smith. Human articular cartilage: Influence of aging and early symptomatic degeneration on the spatial variation of T2–preliminary findings at 3T. *Radiology*, 214:259–266, 2000.

[14] Timothy J. Mosher, Harvey Smith, Bernard J. Dardzinski, Vincent J. Schmithorst, and Michael B. Smith. MR imaging and T2 mapping of femoral cartilage: in vivo determination of the magic angle effect. *American Journal of Roentgenology*, 177:665–669, 2001.

[15] Bernhard Preim, Christian Tietjen, Wolf Spindler, and Heinz Otto Peitgen. Integration of measurement tools in medical 3D visualizations. In *Proceedings of IEEE Visualization 2002*, pages 21–28, 2002.

[16] Harvey E. Smith, Timothy J. Mosher, Bernard J. Dardzinski, Belinda G. Collins, Christopher M. Collins, Qing X. Yang, Vincent J. Schmithorst, and Michael B. Smith. Spatial variation in cartilage of the knee. *J Magn Reson Imaging*, 14:50–55, 2001.

[17] Zsolt Szalavári and Michael Gervautz. The personal interaction panel - a two-handed interface for augmented reality. *Computer Graphics Forum*, 16(3):335–346, 1997.

[18] R. H. van der Rijt, H. van den Bosch, A. Knowles, J. H. Kortman, and J. H. Wondergem. High resolution quantitative imaging of patellar cartilage defects at 1.5T. *Proc. Intl. Soc. Mag. Reson. Med.*, 11:442, 2003.

[19] J. Weese, P. Röche, T. Netsch, T. Blaffert, and M. Quist. Grayvalue based registration of CT and MR images by maximization of local correlation. In *Medical Imaging Computing and Computer-Assisted Intervention MICCAI 1999*, pages 656–663, 1999.